Astron. Astrophys. 334, 1047–1055 (1998)

ASTRONOMY AND ASTROPHYSICS

Bistability in large chemical networks: a global view

H.-H. Lee[1], E. Roueff[2], G. Pineau des Forêts[2], O.M. Shalabiea[1,3], R. Terzieva[4], and Eric Herbst[1,5]

[1] Department of Physics, The Ohio State University, Columbus, OH 43210, USA
[2] DAEC, Observatoire de Paris, F-92195 Meudon Principal Cedex, France
[3] Department of Astronomy, Faculty of Science, Cairo University, Egypt
[4] Department of Chemistry and Chemical Physics Program, The Ohio State University, Columbus, OH 43210, USA
[5] Department of Astronomy, The Ohio State University, Columbus, OH 43210, USA

Received 22 August 1997 / Accepted 29 January 1998

Abstract. The nature of bistability in large gas-phase chemical networks of dense interstellar clouds at 10 K is examined. The dependence of bistability on the parameter $\zeta/n_{\rm H}$, the cosmic ray ionization rate divided by the total hydrogen density, for a wide range of elemental depletions is investigated in detail. We confirm that bistability can exist at steady-state for a range of $\zeta/n_{\rm H}$, but we also confirm that the range of bistability is very dependent on elemental depletions, and also dependent on which network is utilized. In particular, bistability is a more salient feature in the new neutral-neutral model than it is in the new standard model. With the former model, we find that for some gas-phase elemental abundances, the bistability range is non-existent while for others the bistability range includes gas densities as high as 1 10^5 cm^{-3} assuming a standard value for ζ. When all of our new neutral-neutral model results are plotted on one diagram with the fractional electron abundance as ordinate and the parameter $\zeta/n_{\rm H}$ as abscissa, it is found that bistability is confined to a vertical band which is narrower at small $\zeta/n_{\rm H}$ (high densities). Above and below the band lie the so-called "high metal" and "low metal" single-phase results. The intermediate electron abundances at which bistability occurs are best obtained by relatively high abundances of the element sulfur because this element, unlike real metals, is a "soft" ionizer; i.e., its abundance is not totally in ionized forms. We present newly-obtained steady-state results for a variety of molecules in both the HIP (high ionization phase) and LIP (low ionization phase) solutions for a bistable model at a rather high density near 3 10^4 cm^{-3} with a standard cosmic ray ionization rate. Both the steady-state results as well as a variety of early-time results are compared with observations in TMC-1 and L134N.

Key words: ISM: clouds – ISM: abundances – ISM: molecules – molecular processes

1. Introduction

The phenomenon of bistability in gas phase chemical models of interstellar clouds is by now well known (Pineau des Forêts et al. 1992, Le Bourlot et al. 1993, 1995a,b, Shalabiea & Greenberg 1995). The term bistability refers to the existence of two stable steady-state chemical solutions – labelled the high ionization phase (HIP) and the low ionization phase (LIP) – over a certain range of gas densities and cosmic ray ionization rates. The two solutions, obtained both by solution of algebraic equations and by following the time dependence of differential equations until no further changes occur, arise from different initial conditions. In addition to a high degree of ionization, the HIP solution is characterized by a high C/CO abundance ratio, while the LIP solution is characterized by a much lower C/CO abundance ratio. Other chemical differences have also been explored (Gerin et al. 1997). When selected results, such as the C/CO abundance ratio, are plotted against density or cosmic ray ionization rate, the nature of bistability emerges (Flower & Pineau des Forêts 1996). Starting, for example, from high density with initial abundances either rich in molecules or rich in atoms (with the exception of H_2), and proceeding to lower densities at a fixed ionization rate, one encounters only one solution with relatively low ionization at steady-state until at a certain critical point, a sharp phase transition occurs to the HIP solution for the initial abundances rich in atoms. If initial abundances rich in molecules are used, no sharp transition occurs at this density, and a second solution – the LIP solution – is obtained. At a lower density critical point, the LIP solution reached from molecular initial conditions undergoes a phase transition of its own and merges with the HIP solution. At still lower densities, there exists only one solution, with relatively high ionization.

Although the LIP solution corresponds more closely to the "low metal" solution used most frequently by modellers (Lee et al. 1996; the exact correspondence is explored below), the HIP solution offers a plausible explanation for the high atomic carbon abundances observed towards diverse interstellar sources but more commonly explained in terms of photon dominated regions (Keene 1995). In addition, the existence of bistability might help to explain the large abundance variations often seen on small distance scales. One promising line of research concerns differences in deuteration between the LIP and the HIP (Gerin et al. 1997). Although the inclusion of the element deuterium does not have a global effect on the bistability, the

Send offprint requests to: Eric Herbst

HIP and LIP phases show differing abundances of deuterated species. The relevance of bistability to the actual interstellar medium, however, rests on questions such as whether or not it is an artifact of incomplete models and over how wide a region of parameter space it occurs. Bistability has by now been investigated in both small- and moderately-sized model networks, although it has not been studied in any detail with the largest chemical networks, which might be expected to be the most stable. The dependence of the range of bistability on elemental depletions has also been looked at to some degree (Le Bourlot et al. 1995a). In addition, the effect of grain chemistry on the nature of bistability has been investigated and debated (Shalabiea & Greenberg 1995, Le Bourlot et al. 1995b). There is thus still an element of controversy concerning bistability, and a more thorough investigation of the phenomenon is indicated. In this paper, we report such a thorough investigation with a very large gas-phase chemical network – the so-called "new neutral-neutral" model of Bettens et al. (1995). We have chosen not to study bistability with gas-grain model networks at this time, for reasons given in Sect. 4.

Our investigation has been facilitated by the realization (Lepp & Dalgarno 1996), confirmed by us, that steady-state fractional abundances in gas-phase chemical networks where direct photodestruction by external photons can be ignored depend uniquely on the ratio $\zeta/n_{\rm H}$, where ζ (s^{-1}) is the cosmic ray ionization rate and $n_{\rm H}$ is the total hydrogen density ($n({\rm H}) + 2n({\rm H_2})$). In other words, if both ζ and $n_{\rm H}$ are changed by a common factor f, then the steady-state fractional abundances remain unchanged. In discussing steady-state results, we are thus able to use the ratio $\zeta/n_{\rm H}$ to characterize the range of bistability rather than varying each parameter while fixing the other. For non-steady-state results, however, the simple dependence on the ratio $\zeta/n_{\rm H}$ does not pertain, although at the so-called "early time" (where the complex molecule abundances in "low metal" models tend to maximize), the fractional abundances, if not the time taken to reach them, also depend only on the $\zeta/n_{\rm H}$ ratio. Mathematically, the condition for unique dependence on the ratio $\zeta/n_{\rm H}$ is that the time derivatives of the concentrations be zero. Of course, this argument neglects the thermal balance; a high value of ζ is likely to increase the temperature and so cause a change in the chemistry.

2. Chemical models and strategy

The large gas-phase chemical network emphasized in this paper – the "new neutral-neutral model" of Bettens et al. (1995) – includes 409 species and almost 4,000 chemical reactions. The model contains a large selection of rapid neutral-neutral reactions based on an extrapolation of limited low-temperature experimental results (Sims & Smith 1995). The new neutral-neutral model fails to produce sufficiently large abundances of complex molecules at early time to explain observed results in the well-studied source TMC1. A second model of Bettens et al. (1995), the "new standard model", contains far fewer rapid neutral-neutral reactions and produces much larger abundances of complex molecules at early time. We adopt the new neutral-neutral model as the standard model here, since it is physically the more reasonable and since large abundances of complex molecules are not produced in either network with most of the elemental abundances discussed below. Some analogous calculations have been undertaken with the new standard model; differences between the two models relating to bistability are mentioned in the discussion section.

In the use of both networks here, we neglect photodestruction of molecules caused by external photons ($A_v \geq 10$), although we include photodissociation and photoionization induced by secondary UV photons produced by cosmic rays (Gredel 1990). A small but significant change to the networks is the use of the latest storage ring results (Larsson et al. 1993; Sundström et al. 1994) for the temperature dependence and product branching fraction of the dissociative recombination rate coefficient of H_3^+ with electrons; the rate is larger at low temperatures than the rate used by Bettens et al (1995). Specifically, the formula used for the overall rate coefficient k is $1.15\ 10^{-7}$ (T(K)/300)$^{-0.65}$ $cm^3\ s^{-1}$ with a product fraction of 0.75 for the 3H channel and 0.25 for the H_2 + H channel. A large rate ($k \geq 2.5\ 10^{-8}\ cm^3\ s^{-1}$) is well known to be critical for bistability (Le Bourlot et al. 1995a).

For a large number of gas-phase elemental abundances, the region of bistability was elucidated by running two types of models under homogeneous physical conditions at a temperature of 10 K. At Meudon, steady-state calculations were run, while at Columbus, pseudo-time-dependent calculations were run until steady-state conditions were reached. The two methods are in excellent agreement. The time-dependent results were obtained by solving a system of ordinary but non-linear differential equations with the Gear method. The region of bistability (if any) for each set of elemental abundances was determined by plotting the ionization fraction vs the parameter $\zeta/n_{\rm H}$. For each set of elemental abundances, two types of initial conditions (or, in the case of the steady-state calculations, initial guesses) were utilized. With the "atomic" initial conditions, all of the elements other than hydrogen are completely in atomic form. This set corresponds to the typical initial conditions in pseudo-time-dependent models (e.g. Lee et al. 1996). With the "molecular" conditions, the carbon, nitrogen, and oxygen start off in the molecules CO, N_2, and O_2. In the region of bistability, as mentioned previously, the atomic initial conditions lead to the HIP solution and the molecular initial conditions lead to the LIP solution. Outside of the region of bistability, the two sets of initial abundances lead to the same steady-state abundances. Fig. 1 contains a typical plot of fractional ionization vs $\zeta/n_{\rm H}$ in which a bistable region exists; the effect would be just as noticeable if we plotted other results, such as the abundance ratio between C and CO, vs $\zeta/n_{\rm H}$. The vertical lines at the two critical points are to elucidate the bistable region only.

A wide variety of elemental abundances has been used through the years in gas-phase models of dense interstellar clouds. Virtually all have, to a greater or a lesser extent, contained the assumption of depletion of heavy elements to form the dust particles. In diffuse clouds, optical measurements have been used for some time to determine gas-phase elemental abun-

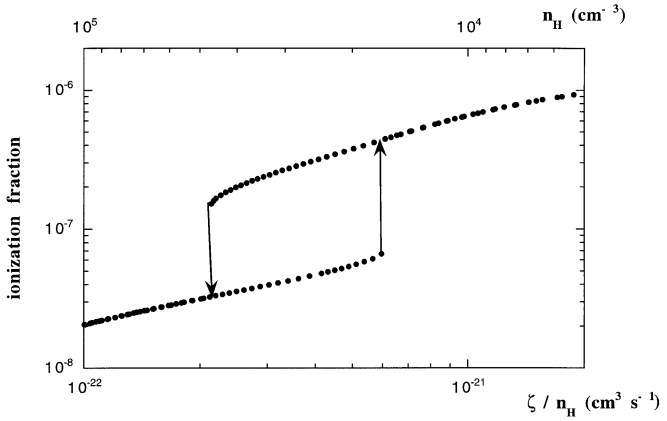

Fig. 1. The phenomenon of bistability at steady state shown by plotting the ionization fraction (with respect to $n_{\rm H}$) vs. $\zeta/n_{\rm H}$. The arrows depict the domain of $\zeta/n_{\rm H}$ where two solutions occur. The upper abscissa scale of density corresponds to $\zeta = 10^{-17}$ s^{-1}. The particular calculation makes use of "low metal" abundances except for a fractional sulfur abundance of 2 10^{-6}.

dances. Early measurements (Morton 1975) showed the elements C, N, and O to be depleted by factors of 6, 2.5, and 4, respectively, from solar values. More recent measurements (Cardelli et al. 1996; Savage & Sembach 1996; Grevesse et al. 1996; Meyer 1997) show somewhat more modest depletions of these elements of 3, 1-2, and 2 respectively, as well as hardly any depletion for S. In addition, Li & Greenberg (1997) have recently used indirect evidence and a so-called unified dust model to discuss elemental depletions in diffuse clouds. In dense clouds, rather modest additional elemental depletions from the gas for C (2.4%), and O(13%), have been derived by Shalabiea & Greenberg (1995) to account for the presence in grain mantles of water and CO.

In this global study, we have used a variety of elemental abundances, which can be regarded as variations of three primary sets of abundances. Two of these sets are the well-known "low metal" and "high metal" abundances (e.g. Leung et al. 1984; Graedel et al. 1982) in which the elements C, N, and O are depleted according to Morton (1975). The "high metal" and "low metal" results differ in abundances for the elements S, Si, Na, Mg, and Fe, with the former containing a modest depletion of 2 for sulfur and stronger depletions of 50, 10, 60, 110, respectively for the other elements while the "low metal" values contain additional depletions of 100 for each. Although the "high metal" abundances give a reasonable description of diffuse cloud gas-phase measurements, the "low metal" results typically yield substantially better agreement with observation in cold dense interstellar clouds (Graedel et al. 1982), without, it would appear, violating any obvious elemental constraints based on gas-phase observations. In addition to these two sets of primary abundances, we have also started with a set of abundances we refer to as the "dense core" abundances. These are derived by Flower et al. (1995) from the solar values of Anders & Grevesse (1989) via an analysis based on a review article by van Dishoeck et al. (1993). Here, near solar abundances are used for N, O, and

Table 1. Solar and primary elemental abundances with respect to total hydrogen

Element	Solar	Dense Core	High Metal	Low Metal
C	3.55(-4)	1.41(-4)	7.30(-5)	7.30(-5)
N	9.33(-5)	1.06(-4)	2.14(-5)	2.14(-5)
O	7.41(-4)	6.72(-4)	1.76(-4)	1.76(-4)
S	1.86(-5)	1.66(-5)	8.00(-6)	8.00(-8)
Si	3.55(-5)	8.00(-9)	8.00(-7)	8.00(-9)
Fe	3.24(-5)	1.50(-8)	3.00(-7)	3.00(-9)
Na	1.9(-6)	2.00(-9)	2.00(-7)	2.00(-9)
Mg	3.80(-5)	7.00(-9)	7.00(-7)	7.00(-9)

Note: the C, N, and O abundances in the "dense core" column are based on the earlier solar values of Anders & Grevesse (1989) which are slightly different from those of Savage & Sembach (1996).

S, while C is depleted from its solar value by a factor of 2-3. As opposed to these non-existent to small depletions, the "dense core" abundances contain only a small amount of true metals (Na, Mg, Fe) so that they resemble the "low metal" abundances *except for a large amount of sulfur*. The gas-phase abundance of sulfur appears to be particularly poorly constrained in dense clouds based on observations to date, which is unfortunate given the primary role of this element in bistability (see below). The three primary sets of abundances are all listed in Table 1 along with solar abundances. Since true metals lead to relatively high levels of ionization and the element sulfur can be regarded as a "soft ionizer", leading to moderate levels of ionization, the three sets of abundances will lead at moderate to high densities ($n \geq$5000 cm^{-3} with "standard" ζ) to fractional ionizations that are relatively low ("low metal" abundances), moderate ("dense core" abundances), and high ("high metal" abundances). After studying the bistability phenomenon using these primary sets of abundances, we then undertook variations, mainly in the element S, to determine their effect on bistability. It should be reiterated that the Meudon group has also used a variety of other elemental abundances in their bistability calculations (Le Bourlot et al. 1993, 1995a).

3. Results

We found that bistability occurs for certain ranges of $\zeta/n_{\rm H}$ for a wide assortment of elemental abundances. However, certain elemental abundances do *not* lead to bistability. The most prominent are abundances with large amounts of actual metals (Na, Mg, Fe). Starting from the "high metal" abundances in Table 1, we varied the S abundance but found bistability under no circumstances. Some relevant results from the steady-state calculations are shown in Fig. 2a, in which fractional ionization is plotted vs both $\zeta/n_{\rm H}$ and $n_{\rm H}$ (assuming $\zeta = 1\,10^{-17}$ s^{-1}.) The other sets of primary abundances in Table 1 do show bistability, as do variations from them, especially in the S abundance. The region of bistability obtained using the "dense core" abundances and variations lies at high $\zeta/n_{\rm H}$ (low densities) for a wide va-

riety of sulfur depletions. With an enhancement in S, however, the region of bistability for the "low metal" abundances lies at surprisingly small $\zeta/n_{\rm H}$ (large densities). Steady-state results for these two cases are shown in Figs. 2b and 2c, respectively.

A global view of our results can be seen in Fig. 3 where we have synthesized many individual results of the type shown in Figs. 1 and 2, with ordinate the fractional ionization and abscissa $\zeta/n_{\rm H}$. Note that for a "typical" value for ζ of $\approx 10^{-17}$ s^{-1}, the densities on the plot range from a low near 10 cm^{-3} to a high near 10^5 cm^{-3} with increasing density going from right to left. In Fig. 3a, the individual results can be seen, while in Fig. 3b the outer borders of the region where bistability occurs are depicted. We have undertaken such a synthesis in the hope that, like the HR diagram, a global figure of this type would be instructive. To make Fig. 3a, we plotted actual points from bistable regions only. Calculations for elemental abundances in which bistability occurred for no range of $\zeta/n_{\rm H}$ as well as the results outside of the bistability range were not plotted. Bistable solutions based on the "low metal" elemental abundances (Table 1) and variations as well as bistable solutions based on the "dense core" abundances and variations are included. It can be seen that for all solutions plotted, bistability occurs in a vertical band of fractional ionization which appears to widen somewhat as one goes from small to large $\zeta/n_{\rm H}$ (large to small gas density). The amount of widening is uncertain since we may expect that at low densities, UV penetration leads to an increase in temperature, an effect that hinders bistability but, at the same time, increases the abundances of C^+ and S^+, which may have the opposite effect.

Within the band of intermediate ionization depicted in Fig. 3b, it is by no means guaranteed that bistability will occur for a given set of abundances, since calculations with individual elemental abundances only go bistable for limited ranges of $\zeta/n_{\rm H}$. Outside of the band, however, we have not been able to find bistability. Above the band at relatively high densities lie the single-phase "high metal" dense cloud solutions whereas below the band at these densities lie the "low metal", low sulfur solutions. These latter solutions pertain to the typical models used at early-times to explain molecular abundances in sources such as TMC-1 (note that the new neutral-neutral model used here fails in this task). The bistable solutions in the band at high density ($10^{3.5-5}$ cm^{-3} with $\zeta = 1\,10^{-17}$ s^{-1}) are for "low metal" elemental abundances with, however, an increased sulfur abundance which results in higher ionization levels. The different points also derive from variations in the C/O elemental abundance ratio. *These high density bistable solutions are new*; previous solutions exist mainly at densities lower than standard dense cloud values unless a high value of ζ is assumed.

We present detailed steady-state results for one such high density bistable solution - obtained with an elemental sulfur fractional abundance of 2 10^{-6} and the other elements held to their "low metal" values. The region of bistability occurs within a range for $\zeta/n_{\rm H}$ of 2.7-6.2 10^{-22} cm^3 s^{-1}, which, with a "standard" value of ζ = 1.3 10^{-17} s^{-1}, corresponds to a density range of 2.1-4.8 10^4 cm^{-3}. Results for both phases at a density of 2.6 10^4 cm^{-3} are listed in Table 2 for species with fractional

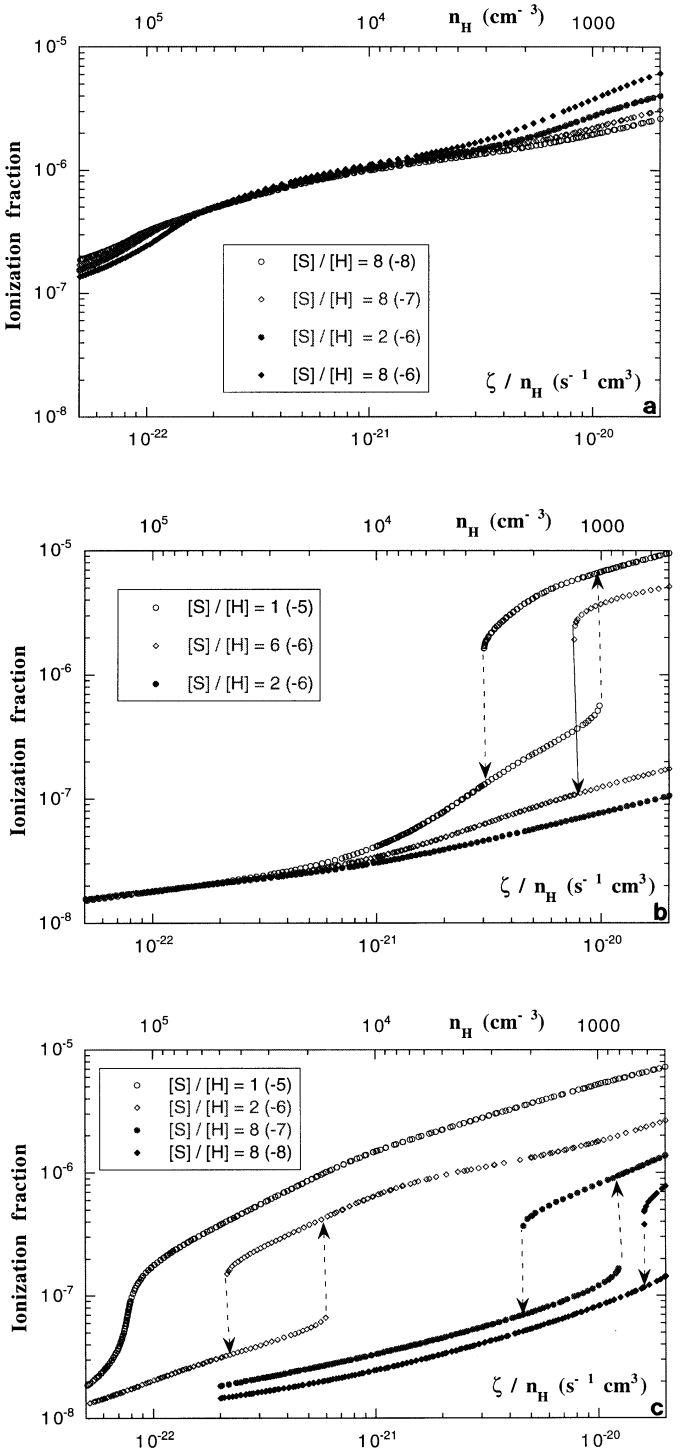

Fig. 2. **a** The ionization fraction plotted vs. $\zeta/n_{\rm H}$ and vs. $n_{\rm H}$ ($\zeta = 10^{-17}$ s^{-1}) for "high metal" abundances and different sulfur depletions. No bistability can be seen. **b** The ionization fraction plotted vs. $\zeta/n_{\rm H}$ and vs. $n_{\rm H}$ ($\zeta = 10^{-17}$ s^{-1}) for "dense core" abundances and different sulfur depletions. Bistability can be seen but only at rather large values of $\zeta/n_{\rm H}$ (low densities). **c** The ionization fraction plotted vs. $\zeta/n_{\rm H}$ and vs. $n_{\rm H}$ ($\zeta = 10^{-17}$ s^{-1}) for "low metal" abundances and different sulfur depletions. Bistability can be seen over a wide range of $\zeta/n_{\rm H}$ values, depending strongly on the sulfur depletion.

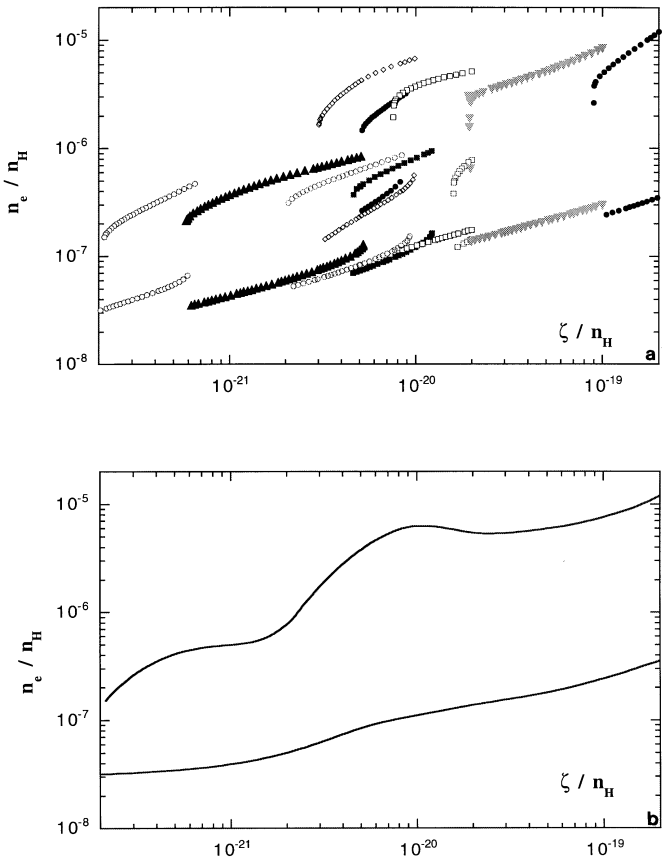

Fig. 3. a A "global" diagram for bistability obtained by superimposing points from the bistability regions of different calculations on a plot with the fractional ionization as the ordinate and $\zeta/n_{\rm H}$ as the abscissa. Both LIP and HIP results for elemental abundances based on the primary "low metal" and "dense core" abundances in Table 1 are depicted. The new neutral-neutral model network has been used. **b** The results of **a** are depicted so that only the outer borders of the region where bistable solutions occur are shown. Above the bistable region at high densities lie the single-phase "high metal" dense cloud solutions while below the band at these densities lie the "low metal", low sulfur solutions.

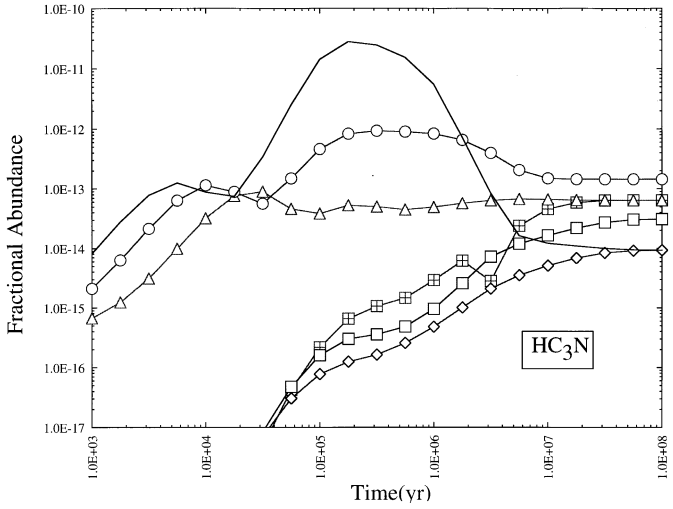

Fig. 4. The relationship between bistability and time dependence is shown for the fractional abundance (with respect to H_2) of the complex molecule HC_3N using the new standard model. Only for atomic initial conditions and values of $\zeta/n_{\rm H}$ below the onset of bistability does a large enhancement at early time occur. The various symbols are defined as follows: the dark solid line and the open diamonds refer, respectively, to atomic and molecular initial conditions with $\zeta/n_{\rm H}$ below the region of bistability; the open circles and the open squares refer, respectively, to the HIP and LIP; the open triangles and the squares divided into four refer, respectively, to atomic and molecular initial conditions with $\zeta/n_{\rm H}$ above the region of bistability

abundances greater than 10^{-12} in at least one phase; these are discussed in the next section.

A similar plot to Fig. 3 with the abundance ratio between C and CO replacing the fractional ionization is not as useful since many "high-metal"-based solutions without bistability lie in the same region as the bistable results.

4. Discussion

4.1. Steady state

Fig. 3 indicates why the gas-phase elemental abundance of sulfur plays such an important role in bistability, especially at high densities. Moderate to high abundances of sulfur lead to moderate electron abundances; it is these moderate electron abundances that are most conducive to bistability. If the electron abundance is too large, as tends to happen with "high metal" elemental abundances (Table 1), bistability cannot exist. A perusal of some "high metal" solutions (Lee et al. 1996) shows that although the abundances of molecular ions such as H_3^+ are driven to lower levels by dissociative recombination, they are still somewhat greater than the abundances of the atomic ions, such as H^+. In this and in other ways (such as the C abundance), the "high metal" solutions are more akin to the LIP solution in the bistability region despite their high ionization fraction. If the electron abundance is very low, which occurs (except at very low gas densities) when "low metal" abundances (including low sulfur) are used, then the molecular ions strongly dominate. Starting with "low metal" elemental abundances at moderate to high densities, and adding sulfur increases the fractional ionization gently, driving down the molecular ionic abundances until a regime is reached in which both the HIP (fractional ionization greater; atomic ions more prominent) and the LIP (fractional ionization smaller; atomic ions less prominent) can seemingly coexist. (Remember that bistability does exist for "low metal" solutions with the sulfur abundance in Table 1 or even with no sulfur at all, but the region of bistability lies at very low densities.) If the sulfur elemental fractional abundance is increased past a value of 3.5 10^{-6} while holding other abundances at the "low metal" values, then bistability can no longer occur, presumably due to too high an ionization fraction. Bistability at low densities can exist with significantly higher sulfur elemental abundances, since it exists for the primary "dense core" abundances; here, presumably, the excess sulfur is balanced in some manner by the low C/O abundance ratio.

Table 2. Fractional LIP and HIP abundances for selected species with respect to H_2 at steady state with $n_H = 2.6 \times 10^4$ cm^{-3} and T = 10 K

Species	HIP	LIP	Species	HIP	LIP
C	1.96(-05)	4.24(-07)	Cl	7.98(-09)	7.88(-09)
Fe	8.74(-10)	1.29(-09)	H	1.80(-04)	1.71(-04)
He	2.80(-01)	2.80(-01)	Mg	2.67(-09)	4.83(-09)
N	3.95(-05)	2.87(-05)	Na	5.75(-10)	1.26(-09)
O	2.25(-04)	1.85(-04)	P	5.73(-09)	5.89(-09)
S	3.18(-06)	3.77(-06)	Si	6.26(-09)	4.66(-09)
C_2	8.25(-11)	5.52(-12)	CH	6.91(-10)	9.60(-11)
CN	3.74(-11)	1.08(-11)	CO	1.26(-04)	1.45(-04)
CS	1.97(-07)	2.32(-08)	H_2	1.00(+00)	1.00(+00)
HCl	1.25(-11)	1.16(-10)	HS	5.01(-10)	9.02(-11)
N_2	1.67(-06)	7.03(-06)	NH	1.16(-11)	8.15(-11)
NO	8.83(-10)	8.99(-09)	NS	1.97(-10)	3.83(-11)
O_2	3.17(-07)	1.03(-05)	OH	2.79(-09)	9.80(-09)
PH	4.00(-12)	2.16(-12)	PN	1.77(-10)	9.05(-11)
PO	2.77(-11)	1.88(-11)	S_2	1.31(-11)	1.17(-11)
SiC	9.82(-12)	2.56(-13)	SiH	3.65(-10)	3.93(-11)
SiN	4.67(-11)	6.65(-12)	SiO	5.77(-09)	1.09(-08)
SiS	2.23(-11)	1.65(-11)	SO	6.58(-09)	9.22(-08)
C_2H	2.10(-11)	6.75(-12)	C_2N	4.26(-12)	1.38(-12)
C_2S	3.91(-10)	2.59(-10)	C_3	1.37(-11)	1.29(-12)
CCO	2.00(-12)	9.68(-13)	CH_2	1.57(-10)	3.04(-11)
CO_2	2.57(-09)	3.97(-08)	H_2O	1.24(-07)	5.17(-07)
H_2S	1.49(-11)	1.38(-10)	HCN	2.11(-10)	3.14(-10)
HCO	1.64(-12)	3.72(-12)	HCS	3.70(-11)	2.54(-11)
HCSi	6.58(-12)	7.51(-14)	HNC	6.68(-11)	2.02(-10)
HNO	1.88(-10)	9.42(-10)	HNSi	7.57(-11)	9.07(-11)
HS_2	5.51(-11)	2.66(-10)	N_2O	7.79(-10)	3.05(-09)
NH_2	2.05(-10)	1.07(-09)	NO_2	3.41(-12)	1.78(-11)
OCN	3.05(-10)	9.85(-10)	OCS	3.70(-09)	1.24(-08)
SiO_2	4.02(-12)	1.76(-11)	SO_2	5.12(-10)	1.91(-08)
C_2H_2	1.64(-10)	9.57(-10)	C_3H	1.28(-11)	3.62(-12)
C_3N	1.69(-12)	4.87(-13)	C_3O	5.26(-12)	1.81(-12)
C_3S	2.87(-11)	1.20(-11)	C_4	3.36(-12)	5.97(-14)
CH_3	3.85(-11)	1.57(-11)	H_2CN	4.52(-12)	1.85(-12)
H_2CO	2.04(-10)	4.65(-10)	H_2CS	2.93(-09)	2.72(-09)
H_2S_2	6.03(-11)	2.67(-10)	NH_3	2.39(-11)	9.86(-10)
CH_2CO	4.04(-11)	6.23(-11)	C_2H_3	3.41(-12)	9.48(-13)
C_3H_2	3.09(-12)	4.08(-12)	HCOOH	7.49(-12)	4.15(-10)
CH_4	1.88(-08)	5.28(-08)	CH_3OH	4.08(-12)	1.81(-11)
e	6.49(-07)	1.07(-07)	C^+	1.81(-08)	4.29(-09)
Fe^+	5.12(-09)	4.71(-09)	H^+	1.34(-09)	8.30(-10)
He^+	3.42(-10)	2.87(-10)	Mg^+	1.13(-08)	9.17(-09)
N^+	1.99(-12)	5.78(-12)	Na^+	3.42(-09)	2.74(-09)
P^+	5.82(-11)	4.29(-12)	S^+	6.06(-07)	7.97(-08)
Si^+	3.44(-09)	2.63(-10)	HS^+	7.91(-12)	5.67(-11)
NO^+	1.61(-13)	2.42(-12)	NS^+	1.05(-12)	8.87(-12)
O_2^+	8.43(-13)	1.01(-10)	SO^+	6.88(-11)	4.09(-10)
H_2S^+	9.80(-12)	5.12(-12)	H_3^+	6.97(-10)	1.16(-09)
HCO^+	2.17(-10)	2.41(-09)	HCS^+	7.46(-11)	3.22(-11)
$HSiO^+$	6.82(-12)	3.13(-11)	HSO^+	3.34(-13)	7.61(-11)
N_2H^+	8.59(-13)	2.38(-11)	OCS^+	1.18(-11)	2.60(-11)

The role of sulfur in providing regimes of moderate ionization seems central to bistability. Can other elements take the place of sulfur? Certainly, at very low densities (right side of Fig. 3), there is sufficient ionization from elements such as C that no sulfur at all is needed for bistability. At higher densities, we have varied the abundance of Si and of the metals Na, Mg,

Table 2. (contitnued)

Species	HIP	LIP	Species	HIP	LIP
SiH_2^+	1.62(-12)	5.87(-13)	CH_3^+	1.10(-11)	5.26(-12)
H_3O^+	3.00(-11)	3.20(-10)	$HOCS^+$	4.36(-14)	2.36(-12)
HSO_2^+	5.65(-15)	2.02(-12)	$C_2H_3^+$	4.45(-13)	1.13(-12)
H_3CS^+	7.71(-13)	2.01(-12)	NH_4^+	1.26(-13)	4.68(-12)
CH_5^+	1.89(-12)	3.57(-12)	$GRAIN^-$	2.63(-12)	2.63(-12)

Note: "Low metal" abundances except for sulfur, for which a fractional abundance of 2 10^{-6} is used. The density in the heading occurs with a "standard" value for ζ. See text.

and Fe to determine the effect on bistability. We find that an increase of one order of magnitude of the true metals from their "low metal" abundances permits bistability if and only if the sulfur fractional abundance is kept below 8 10^{-7}. In addition, the range of bistability is decreased relative to the low metal models and is shifted to somewhat higher densities. No truly high density regions of bistability exist. An increase of two orders of magnitude, as noted above, (which brings the metallic abundance to their "high metal" values) kills bistability completely. If one starts with the "low metal" abundances, and increases the abundance of Si, a similar effect occurs to an increase in the true metals; Si is also more efficient at ionization than is S.

The specific results for the high density LIP and HIP solutions in Table 2, obtained with "low metal" abundances except for a sulfur fractional abundance of 2 10^{-6}, show that neither phase exhibits large abundances of polyatomic molecules. The abundances of some molecules are higher in the HIP and of others are higher in the LIP. Those higher in the HIP tend to be small carbon-bearing radicals. In addition, for many molecules, the differences are quite small (a factor of ≈ 3 or less). The phases are, as usual, distinguished by differences in ionization; the HIP level of ionization is due mainly to ionized sulfur. A major result is that the steady-state fractional abundance of atomic C in the HIP is high (2 10^{-5} with respect to H_2), despite the high density of the gas, for normal values of ζ. Such a solution may indeed be applicable to observations of large abundances of C in some physical situations. In particular, Schilke et al. (1995) have shown that at least some fraction of the atomic C detected towards TMC-1 is not just in an outer boundary layer and is reasonably explained by an HIP solution, albeit at densities only up to $n(H_2)$ = 2000 cm^{-3}. The spatial regions modelled by the HIP phase would then not be the higher density region where the large molecules tend to have peak abundances (e.g. TMC-1(CP)). The solutions listed in Table 2 refer to a higher density region (assuming a standard cosmic-ray ionization rate); nevertheless, it is instructive to compare the solutions with some observed abundances.

In Table 3 we have listed observed fractional abundances in the dark clouds TMC-1 and L134N for some small molecules as well as the complex species HC_3N and HC_7N and, in the case of TMC-1, atomic C. We have also listed the analogous calculated abundances for the steady-state (SS) HIP and LIP solutions in Table 2. In past work, we have found that discriminators between the HIP and LIP solutions include the simple carbon-bearing radicals (CH, C_2H, C_3H), sulphur-containing molecules (CS, SO, SO_2) and molecular ions such as HCO^+ and N_2H^+, in the sense that abundance differences between the two phases are usually noticeable. In addition to these species, we have also included NO, OH, and NH_3 in Table 3. As can be seen in the table, neither set of steady-state solutions to the new neutral-neutral model network represents the small molecule abundances observed in TMC-1 or L134N particularly well. The strongest argument in favor of the HIP solution remains the high atomic carbon abundance in TMC-1 observed by Schilke et al. (1995); this and other solutions favoring the HIP are listed in boldface in Table 3. Although the HIP shows higher abundances of the carbon-bearing radicals (CH, C_2H, C_3H) than does the LIP, presumably due to the influence of atomic C, the calculated abundances are still below the observed values. For the other molecules on the list, only perhaps SO is better fit by the HIP phase since the LIP phase overproduces it.

Unfortunately, calculated molecular abundances are model and time dependent; the abundances of polyatomic molecules are generally higher in the new standard model, especially at early time. Also, we have only listed the results of one bistable model; many others are available. Still, the qualitative conclusion that the abundances of many polyatomic molecules are low in bistable regions seems secure.

The results of the new standard model generally show smaller regions of bistability, proving that the phenomenon is, at this stage of understanding, dependent on model network. The region of bistability is particularly reduced for elemental abundances based on the "low metal" abundances (Table 1). In fact, with these primary abundances, no bistability is seen at all. Even when the sulfur abundance is increased, bistability is seen only if the C/O elemental abundance ratio is set lower than the 0.4 value of the "low metal" case (in analogy with the "dense core" abundances). In the cases where bistability is seen, its range in terms of $\zeta/n_{\rm H}$ is considerably smaller than with the new neutral-neutral model. There is no simple explanation for the difference between networks in terms of differing fractional ionizations.

Ruffle et al. (1997) have recently pointed out that depletions of elements such as C, N, and O from the range of values considered here can actually increase abundances of complex molecules such as HC_3N at late times. With depletions for C,

Table 3. Comparison of steady-state (SS) and early-time (ET) HIP and LIP abundances with respect to H_2 with observed fractional abundances in TMC-1 and L134N

Species	TMC-1	L134N	HIP SS	LIP SS	HIP ET	LIP ET	HIP′ ET	LIP′ ET
C	$\approx 1(-05)$	–	$\mathbf{2.0(-05)}$	$4.2(-07)$	$\mathbf{1.1(-04)}$	$1.7(-08)$	$5.6(-06)$	$4.9(-06)$
CH	$2(-08)$	$1(-08)$	$\mathbf{6.9(-10)}$	$9.6(-11)$	$\mathbf{1.9(-09)}$	$6.7(-11)$	$5.5(-10)$	$5.0(-10)$
C_2H	$5(-08)$	$5(-08)$	$\mathbf{2.1(-11)}$	$6.8(-12)$	$\mathbf{1.4(-10)}$	$6.6(-13)$	$8.4(-11)$	$7.8(-11)$
C_3H	$5(-10)$	$3(-10)$	$\mathbf{1.3(-11)}$	$3.6(-12)$	$\mathbf{1.2(-10)}$	$1.3(-13)$	$8.3(-11)$	$7.6(-11)$
NO	$3(-08)$	$6(-08)$	$8.8(-10)$	$9.0(-09)$	$5.7(-10)$	$3.6(-09)$	$9.0(-09)$	$9.4(-09)$
OH	$3(-07)$	$3(-08)$	$2.8(-09)$	$9.8(-09)$	$2.8(-09)$	$4.1(-08)$	$1.0(-08)$	$1.0(-08)$
NH_3	$2(-08)$	$2(-07)$	$2.4(-11)$	$1.0(-09)$	$1.5(-11)$	$1.5(-08)$	$1.7(-10)$	$1.8(-10)$
CS	$1(-08)$	$1(-09)$	$2.0(-07)$	$2.3(-08)$	$1.6(-06)$	$5.6(-08)$	$6.1(-08)$	$5.8(-08)$
SO	$5(-09)$	$2(-08)$	$\mathbf{6.6(-09)}$	$9.2(-08)$	$\mathbf{4.6(-09)}$	$1.7(-06)$	$1.2(-07)$	$1.3(-07)$
SO_2	$1(-09)$	$4(-09)$	$5.1(-10)$	$1.9(-08)$	$2.3(-10)$	$3.7(-08)$	$3.4(-08)$	$3.7(-08)$
HC_3N	$6(-09)$	$2(-10)$	$1.0(-13)$	$1.6(-13)$	$\mathbf{1.2(-12)}$	$1.3(-15)$	$6.8(-12)$	$6.5(-12)$
HC_7N	$1(-09)$	$2(-11)$	$9.0(-20)$	$1.6(-19)$	$\mathbf{3.8(-17)}$	$5.0(-24)$	$7.9(-16)$	$9.3(-16)$
HCO^+	$8(-09)$	$8(-09)$	$2.2(-10)$	$2.4(-09)$	$1.1(-10)$	$5.3(-09)$	$2.6(-09)$	$2.7(-09)$
N_2H^+	$5(-10)$	$5(-10)$	$8.6(-13)$	$2.4(-11)$	$2.1(-13)$	$1.3(-10)$	$7.9(-13)$	$8.3(-13)$

Notes: The observed fractional abundances are from Ohishi et al. (1992) except for the estimated C abundance in TMC-1, which is from Schilke et al. (1995). The theoretical abundances are from the model used for Table 2. The boldface theoretical abundances are for those instances in which the HIP solution is superior to the LIP solution. The first two early-time solutions used have atomic and molecular initial conditions respectively, while the third and the fourth ones have atomic initial conditions with the exception of oxygen, 82% and 83% of which is, respectively, molecular in form. The early-time abundances listed are for 5.6 10^4 yr.

N, and O of a factor of 5 from the low metal abundances, we confirm this effect, and, using the new neutral-neutral model, note that the bistability at 10 K vanishes.

4.2. Time dependence

No mention so far has been made of early-time bistable solutions in our time-dependent calculations. Early-time solutions show large enhancements for large molecules with "low metal" abundances and with atomic starting conditions for all species other than H_2 (Herbst & Leung 1989; Lee et al. 1996). We have looked at early-time solutions in some detail. For solutions showing bistability at steady state, there are no large early-time enhancements in either the LIP or the HIP with our given atomic and molecular initial abundances. The situation is depicted in Fig. 4 for the molecule HC_3N with the new standard model and the "dense core" abundances. With a value of $\zeta/n_{\rm H}$ low enough (4 10^{-21} cm^3 s^{-1}) such that only a low ionization solution is found, it can be seen that a large early time solution exists for atomic initial conditions but not for molecular initial conditions (high in CO and O_2) since in the latter case, no free carbon is available to make complex species. Both solutions are the same at steady state. When $\zeta/n_{\rm H}$ is increased into the bistable region (8 10^{-21} cm^3 s^{-1}), atomic initial conditions lead to the HIP and molecular initial conditions lead to the LIP; both sets of solutions show no large peak at early time although the atomic initial conditions lead to a small early-time enhancement. When $\zeta/n_{\rm H}$ is increased still further (2 10^{-20} cm^3 s^{-1}) so that only a high ionization solution can be reached, both atomic and molecular initial conditions show no early-time enhancement at all.

The slight enhancement for HC_3N at early time in the bistable region when atomic initial conditions are used suggests that the excess C in this solution is indeed feeding through partially to carbon-bearing species, and that carbon-bearing species might in general be more abundant at early time. For the species listed in Table 3, we have also tabulated their calculated early-time abundances for solutions leading to both the HIP (atomic initial conditions) and LIP (molecular initial conditions). The model used is the same one used to produce Table 2; viz, the new neutral-neutral model at high density with a standard ζ, plus "low metal" abundances except for enhanced sulfur. It can be seen that there is an enhancement in the abundances of the carbon-bearing species relative to the steady-state HIP values. With the enhancement, the agreement between these species and observation in both TMC-1 and L134N improves somewhat, but is still not as good as obtained with that obtained using low ionization models outside of the zone of bistability (see Fig. 3).

We have also considered the time-dependent chemistry for bistable solutions starting from a variety of initial abundances in between our standard atomic and molecular initial conditions used to derive the results in Tables 2 and 3. We reemphasize the point that we are *not* varying the elemental abundances but are varying the initial atomic and molecular forms in which the "low metal" + high sulfur elemental abundances are grouped. There are two issues here to be investigated: (a) which sets of initial abundances lead to which phase at steady state, and (b) whether

or not early-time abundances can be significantly changed by changing the initial abundances.

Regarding issue (a) we have found the initial presence of at least some molecular oxygen to be a necessary condition for an LIP solution at steady state. Specifically, such a solution is obtained even for initial abundances rich in heavy atoms except oxygen, if 82.3% or more of the oxygen is molecular. For initial abundances with molecules other than O_2 such as CO and/or N_2, the necessary amount of O_2 to achieve an LIP solution can be significantly smaller. If all C is initially in the form of CO and N in the form of N_2, the LIP is obtained with at least 2% of the remaining O in the form of O_2. If 10% of the carbon is in the form of C and 90% in the form of CO, it takes 12% of the remaining oxygen in the form of O_2 to obtain the LIP solution.

Regarding issue (b) we have found the early-time abundances to be very sensitive to changes in the initial abundances, as previously discussed by Flower & Pineau des Forêts (1996). Despite the complexity, a large initial abundance of atomic C generally leads to some enhancement in the early-time abundances of carbon-bearing species, as is to be expected. To give a flavor for the variability obtainable in early-time abundances, we have considered two sets of initial conditions close to the so-called "separatrix", which divides those sets of initial conditions leading to different (bistable) results. Specifically, we started with initial abundances rich in atoms with the exception of oxygen, for which we used 82% (leading to the HIP) and 83% (leading to the LIP) respectively in the form of molecular oxygen. Initial conditions close to the separatrix are known to increase the time needed to achieve bifurcated results. Some early-time abundances from these two sets of initial conditions are shown in Table 3; the columns for these particular solutions are labelled by primes and the designations HIP and LIP, which refer to the final results. Although the two solutions do bifurcate later into the standard LIP and HIP solutions, they show very little difference at all at early time ($5.6\ 10^4$ yr). In both of the early-time solutions, there are moderate enhancements in the abundances of carbon-bearing species, due presumably to the high abundance of C in both phases. As regards the agreement with observed abundances in TMC-1 and L134N, these high density, early-time solutions do not lead to sufficient cyanopolyynes, carbon-bearing species, and ammonia, but do yield high atomic C values.

A final point of discussion concerns the effect of including dust chemistry on the phenomenon of bistability. This has already been discussed in the literature by Shalabiea & Greenberg (1995) and by Le Bourlot et al. (1995b). In the interim, we have confirmed the result of Tielens (lecture, 1995; see also Charnley et al. 1997; Tielens & Charnley 1997) that the rate equations used in standard models of interstellar dust chemistry do not adequately take the finite size of dust particles into account. We have modified the rate equations (Caselli et al. 1998), and tested their effects on standard gas-grain models (Shalabiea, Caselli, & Herbst 1998). The question of bistability can now be tackled.

Acknowledgements. E. H. acknowledges the support of the the National Science Foundation for his research program in astrochemistry. He also thanks the Ohio Supercomputer Center for time on their Cray YMP-8 machine, without which the time-dependent calculations would not have been possible. We are indebted to the referee for many useful comments.

References

Anders E., Grevesse N., 1989, Geochim. Cosmochim. Acta 53, 197
Bettens R. P. A., Lee H.-H., Herbst E., 1995, ApJ 443, 664
Cardelli J. A., Meyer D. M., Jura M., Savage B. D., 1996, ApJ 467, 334
Caselli, P., Hasegawa, T. I., Herbst, E., 1998, ApJ 495, 309
Charnley S. B., Tielens A. G. G. M., Rodgers S. D. , 1997, ApJ 482, L203
Flower D., Pineau des Forêts G., 1996, Physics World 9, 37
Flower D., Pineau des Forêts G., Walmsley C. M., 1995, A&A 294, 815
Gerin M., Falgarone E., Joulain K., Kopp M., Le Bourlot J., Pineau des Forêts G., Roueff, E., Schilke, P., 1997, A&A 318, 579
Graedel T. E., Langer W. D., Frerking M. A., 1982, ApJS 48, 321
Gredel R., 1990, in: Harquist T. W. (ed.) Molecular Astrophysics, Cambridge University Press, p. 305
Grevesse N., Noels A., Saural A. J., 1996, in: Holt S. S., Sonneborn G. (eds) Cosmic Abundances, ASP Conf. Series 99, 117
Herbst E., Leung C. M., 1989, ApJS 69, 271
Keene J. 1995, in: Winnewisser G., Pelz G. C. (eds) The Physics and Chemistry of Interstellar Molecular Clouds, Springer, Berlin, p. 186
Larsson M., Danared H., Mowat J.R., Sigray P., Sundström G., Broström L., Filevich A., Källberg A., Mannervik S., Rensfelt K.G., Datz S., 1993, Phys. Rev. Let. 70, 430
Le Bourlot J., Pineau des Forêts G., Roueff E., 1993, ApJ 416, L87
Le Bourlot J., Pineau des Forêts G., Roueff E., 1995a, A&A 297, 251
Le Bourlot J., Pineau des Forêts G., Roueff E., 1995b, A&A 302, 870
Lee H.-H., Bettens R. P. A., Herbst E., 1996, A&A Suppl. 119, 1
Lepp S., Dalgarno A., 1996, A&A 306, L21
Leung C. M., Herbst E., Huebner W. F., 1984, ApJS, 56, 23
Li A., Greenberg J. M. 1997, A&A 323, 566
Meyer D. M., 1997, in: van Dishoeck, E. (ed) Molecules in Astrophysics: Probes & Processes, Kluwer, Dordrecht, p. 407
Morton D. C., 1975, ApJ 197, 85
Ohishi M., Irvine W. M., Kaifu N., 1992, in: Singh, P. D. (ed) Astrochemistry of Cosmic Phenomena, Kluwer, Dordrecht, p. 171
Pineau des Forêts G., Roueff E., Flower D. R., 1992, MNRAS 258, 45
Ruffle D. P., Hartquist T. W., Taylor S. D., Williams D. A., 1997, MNRAS, 291, 235
Savage B. D., Sembach K. R., 1996, Ann. Rev. As. Astr. 34, 279
Schilke P., Keene J., Le Bourlot J., Pineau des Forêts G., Roueff E., 1995, A&A 294, L17
Shalabiea O. M., Caselli P., Herbst E., 1998, ApJ, in press
Shalabiea O. M., Greenberg J. M., 1995, A&A 296, 779
Sims I. R., Smith I.W. M., 1995, Ann. Rev. Phys. Chem. 46, 109
Sundström G. et al., 1994, Science 263, 785
Tielens A. G. G. M., Charnley, S. B., 1997, Origins of Life and Evolution of the Biosphere, 27, 34
van Dishoeck E., Blake G. A., Draine B. T., Lunine J. I., 1993, in: Levy E. H., Lunine J. I. (ed.) Protostars and Planets III, p. 163